IL NUOVO CIMENTO **47 C** (2024) 12
DOI 10.1393/ncc/i2024-24012-5

Colloquia: La Thuile 2023

Inclusive and differential $\sigma_{t\bar{t}}$ measurements using the ATLAS detector

L. Martinelli(1)(2) on behalf of the ATLAS Collaboration

(1) *Dipartimento di Fisica, Sapienza Università di Roma - Roma, Italy*
(2) *INFN, Sezione di Roma1 - Roma, Italy*

received 10 October 2023

Summary. — Measurements of the total and differential top-quark pair-production cross-sections in proton proton collisions at 13 TeV with the ATLAS detector at the Large Hadron Collider (LHC) are presented. The measurements use data collected by ATLAS during the entire LHC Run 2 (2015 - 2018) corresponding to an integrated luminosity of 140 fb^{-1}. The measurements are performed in the di-lepton channel, requiring an opposite-charge high-p_T electron-muon pair and b-tagged jets. The experimental uncertainties due to the identification of b-quark jets are constrained in-situ by data. The total cross-section is compared to predictions by theoretical QCD calculations at next-to-next-to-leading (NNLO) order. Absolute and normalised single- and double-differential cross-sections are calculated as a function of single-lepton and dilepton kinematic variables, featuring finer granularity and extended kinematic range compared to previous ATLAS measurements. The results are compared with multiple predictions from next-to-leading-order QCD matrix-element generators matched with parton-shower generators.

1. – Introduction

A new measurements of the top-quark pair-production cross-section ($\sigma_{t\bar{t}}$) with an high precision can be used to test the Standard Model predictions and search for the presence of new physics beyond Standard Model.

Due to its large cross-section, the $t\bar{t}$ process is one of the main background of many analyses. A measurements of the differential cross-section may be used by theorists to tune the Monte Carlo (MC) in order to achieve a better description of the process. A better knowledge of process shapes leads to a more controlled background for the other analyses and then a better precision.

The ATLAS experiment [1] pushed the precision on the measured cross-section down to 1.8% [2]. The totality of the Run 2 dataset of 140 fb^{-1} collected at 13 TeV proton-proton collision energy in 2015-2018 is used [3]. In the selection, an electron-muon pair of opposite-sign charge is required along with jets, of which either one or two are b-tagged.

2. – Analysis strategy

The total fiducial cross-section is found experimentally using an event count technique, called double tagging technique, in the one and two b-tagged jets regions. The two equation that describes the number of events in these two regions are:

$$\begin{aligned} N_1 &= \mathcal{L}\sigma^{\text{fid}}_{t\bar{t}} G_{e\mu} 2\varepsilon_b(1-\varepsilon_b C_b) + N_1^{\text{bkg}} \\ N_2 &= \mathcal{L}\sigma^{\text{fid}}_{t\bar{t}} G_{e\mu} (\varepsilon_b)^2 C_b + N_2^{\text{bkg}} \end{aligned} \tag{1}$$

in which

- $N_{1,2}$ are the total number of events in the opposite sign and opposite flavour di-lepton $e\mu$ channel for 1 b-tagged jet and 2 b-tagged jets respectively;
- $\mathcal{L}$ is the luminosity;
- $\sigma^{\text{fid}}_{t\bar{t}}$ is the fiducial cross-section (the cross-section within the selections);
- ε_b is the b-tagging efficiency;
- C_b is the b-tagging correlation coefficient;
- $G_{e\mu} = N^{\text{reco}}_{e\mu}/N^{\text{particle}}_{e\mu}$ is the lepton reconstruction efficiency;
- $N^{\text{bkg}}_{1,2}$ are the total number of background events in the opposite sign and opposite flavour di-lepton $e\mu$ channel for 1 b-tagged jet and 2 b-tagged jets respectively.

To extract the total inclusive cross-section an additional correction is needed:

$$\sigma_{t\bar{t}} = A_{e\mu} \cdot \sigma^{\text{fid}}_{t\bar{t}} \tag{2}$$

where $A_{e\mu} = N^{\text{particle}}_{e\mu}/N^{all}_{e\mu} \cdot 1/BR(t\bar{t} \to e\mu)$ represents the fraction of $t\bar{t}$ events which have a true $e\mu$ pair (including where one or both leptons are produced via leptonic decays) within the detector and kinematic acceptance (fiducial region).

The two unknown variables in these equations, the cross-section and the combined selection and b-tagging efficiency, are determined with a log-likelihood fit.

The MC contributions are normalised to the integrated luminosity of the data. The observed and predicted yields agree within 1%–2%, as shown in fig. 1.

Eight leptonic differential distributions are taken into consideration in this analysis: $\mathrm{p}_{\mathrm{T}}^{e\mu}$, $\mathrm{p}_{\mathrm{T}}^{l^+}+\mathrm{p}_{\mathrm{T}}^{l^-}$, $\mathrm{p}_{\mathrm{T}}^{l}$, E^e+E^μ, $m^{e\mu}$, $|\eta^l|$, $\Delta\phi^{e\mu}$ and $|y^{e\mu}|$ together with four double differential distributions: $|y^{e\mu}| : m^{e\mu}$, $\Delta\phi^{e\mu} : m^{e\mu}$, $\Delta\phi^{e\mu} : \mathrm{p}_{\mathrm{T}}^{e\mu}$ and $\Delta\phi^{e\mu} : E^e+E^\mu$. Each distribution is unfolded to particle-level in the fiducial region by applying the double tagging technique on each bin of each distribution.

3. – Results

3·1. *Inclusive and fiducial cross-section.* – Inclusive and fiducial cross-section together with single- and double-differential cross-section were measured using the 140 fb^{-1} collected by the ATLAS experiment during the Run 2 period (2015-2018). The measured $t\bar{t}$ cross-section in the fiducial volume is:

$$\sigma^{\text{fid}}_{t\bar{t}} = 10.53 \pm 0.02\ (\text{stat}) \pm 0.13\ (\text{syst}) \pm 0.10\ (\text{lumi}) \pm 0.02\ (\text{beam})\ \text{pb}$$

while the total inclusive $t\bar{t}$ production cross-section is:

$$\sigma_{t\bar{t}} = 829 \pm 1\ (\text{stat}) \pm 13\ (\text{syst}) \pm 8\ (\text{lumi}) \pm 2\ (\text{beam})\ \text{pb},$$

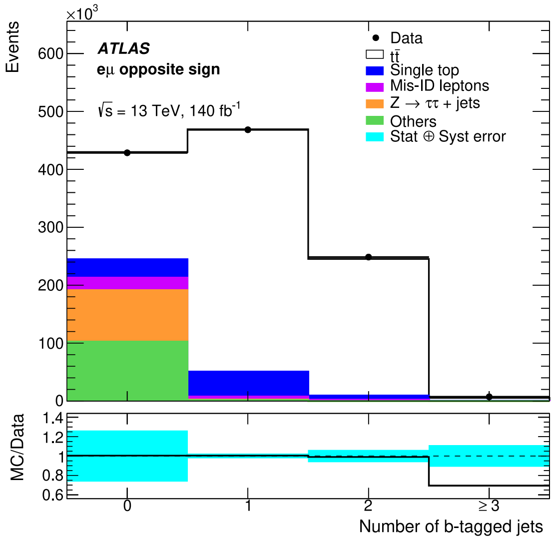

Fig. 1. – Distribution of the number of b-tagged jets in selected opposite-sign $e\mu$ events [2]. The coloured distributions show the breakdown of the predicted background contributions from single top quarks (Wt and t-channel), misidentified leptons, $Z(\rightarrow \tau\tau)+$jets and other sources of background (diboson, $t\bar{t}W$, $t\bar{t}Z$, and $t\bar{t}H$). The bottom panel shows the ratio of the prediction to the data with an uncertainty band covering both the statistical and systematic uncertainties, except for $t\bar{t}$ generator uncertainties [2].

where the uncertainties are, respectively, statistical, systematics, luminosity and, beam energy related. This measurement is the best measurement of the $\sigma_{t\bar{t}}$ at the $\sqrt{s} = 13$ TeV performed so far. It has a smaller relative error with respect to the previous measurements from ATLAS [4, 5] and CMS [6, 7] and it is in agreement with the NNLO prediction [8] of 834^{+21}_{-30} (scale)$^{+21}_{-23}$ (PDF+α_{S}) $\pm\, 23$ (mass) *pb*.

The present measurement is systematically limited. The main systematic uncertainty comes from the luminosity which contributes with 0.93% respect to a total relative uncertainty of 1.8%.

3˙2. *Differential cross-section.* – The results for two differential cross-section are presented in fig. 2. The statistical uncertainty (shown in orange) increases with increasing $\mathrm{p_T}$, combined mass or energy, reaching a maximum of 6%, while it stays constant in η and ϕ. The systematics uncertainty are dominant in these measurements in most of the bins and the biggest source of uncertainty is the luminosity.

3˙3. *Test of the goodness of different generators.* – The level of agreement for the differential cross-section measurements is quantified by calculating χ^2 values according to:

$$\chi^2 = V^T C^{-1} V \tag{3}$$

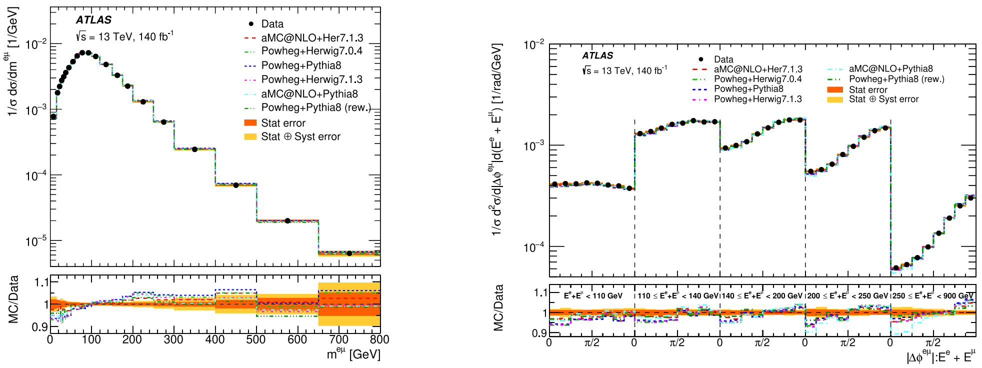

Fig. 2. – Normalised single - and double-differential cross-sections as a function of (a) $m^{e\mu}$ and (b) $|\Delta\phi^{e\mu}|$ in bins of $E^e + E^\mu$ with statistical (orange) and statistical plus systematic uncertainties (yellow) [2]. The data points are placed at the centre of each bin. The results are compared with the predictions from different Monte Carlo generators normalised to the Top++ prediction [8]. The lower panel shows the ratios of the predictions to data, with the bands indicating the statistical and systematic uncertainties. The highest $E^e + E^\mu$ and $\mathrm{p_T}$ bin contains the overflows [2].

where V is the vector of residuals between the measured and predicted cross-sections and C is the covariance matrix of the measured data (including both the statistical and systematic uncertainties). In table I the results for the single-differential measurements are shown.

Table I. – *χ^2 values for the comparison of the normalised measured differential cross-sections with different $t\bar{t}$ simulation samples* [2]. *N_{dof} is the number of degrees of freedom. PP8 corresponds to POWHEG+PYTHIA8 samples, aMCP8 to the aMC@NLO+PYTHIA8 sample, PH704 to the POWHEG+HERWIG7.0.4 while PH713 to the POWHEG+HERWIG7.1.3. The χ^2 values are displayed to one decimal place if the corresponding χ^2 probability is greater than 1%, and rounded to integers otherwise* [2].

Generator N_{dof}	$\mathrm{p_T^\ell}$ 9	$\lvert\eta^\ell\rvert$ 23	$\mathrm{p_T^{e\mu}}$ 9	$\mathrm{p_T^e + p_T^\mu}$ 10	$E^e + E^\mu$ 14	$m^{e\mu}$ 20	$\lvert\Delta\phi^{e\mu}\rvert$ 29	$\lvert y^{e\mu}\rvert$ 29
PP8	196	132	12.0	130	33	102	193	47
PP8 - top $\mathrm{p_T}$ rew.	51	114	7.8	42	20.4	53	65	45.2
PP8 - h_{damp} x 2	228	139	26	167	38	97	121	45.3
PP8 - PDF4LHC	186	100	11.5	125	32	93	185	33.6
PP8 - ISR up	149	111	17.3	120	34	79	66	50
PP8 - ISR down	216	159	10.6	131	30	113	311	44.5
PP8 - Rad up	164	115	27	139	38	78	49	47.6
PP8 - Rad down	216	159	10.6	131	30	113	311	44.5
PP8 - FSR up	216	132	12.5	143	35	106	194	46.8
PP8 - FSR down	171	139	9.5	118	30	98	185	49
PP8 - MEC off	42	136	41	37	16.5	83	181	42.7
aMCP8	16.5	126	48	14.4	14.3	89	300	50
aMCH704	98	137	24	74	24.1	29.1	110	54
PH704	113	104	28	82	28	135	271	45.8
PH713	101	107	31	75	25.5	138	259	45.5

As shown in table I, only few generators have a good description of the data and for some variables no generator can describe the data with a non negligible probability. In addition, no generator can describe the data in double differential distributions [2].

REFERENCES

[1] ATLAS Collaboration, *JINST*, **3** (2008) S08003.
[2] ATLAS Collaboration, *JHEP*, **07** (2023) 141, arXiv:2303.15340 [hep-ex].
[3] ATLAS Collaboration, *Luminosity determination in pp collisions at* $\sqrt{s} = 13$ *TeV using the ATLAS detector at the LHC*, to be published in *Eur. Phys. J. C*, arXiv:2212.09379 [hep-ex].
[4] ATLAS Collaboration, *Eur. Phys. J. C*, **80** (2020) 528, arXiv:1910.08819 [hep-ex].
[5] ATLAS Collaboration, *Phys. Lett. B*, **810** (2020) 135797, arXiv:2006.13076 [hep-ex].
[6] CMS Collaboration, *Eur. Phys. J. C*, **79** (2019) 368, arXiv:1812.10505 [hep-ex].
[7] CMS Collaboration, *Phys. Rev. D*, **104** (2021) 092013, arXiv:2108.02803 [hep-ex].
[8] Czakon M. and Mitov A., *Comput. Phys. Commun.*, **185** (2014) 2930, arXiv:1112.5675 [hep-ph].